Chapter 6

Effect of Functionalization on Electrospun PVDF Nanohybrid for Piezoelectric Energy Harvesting Applications

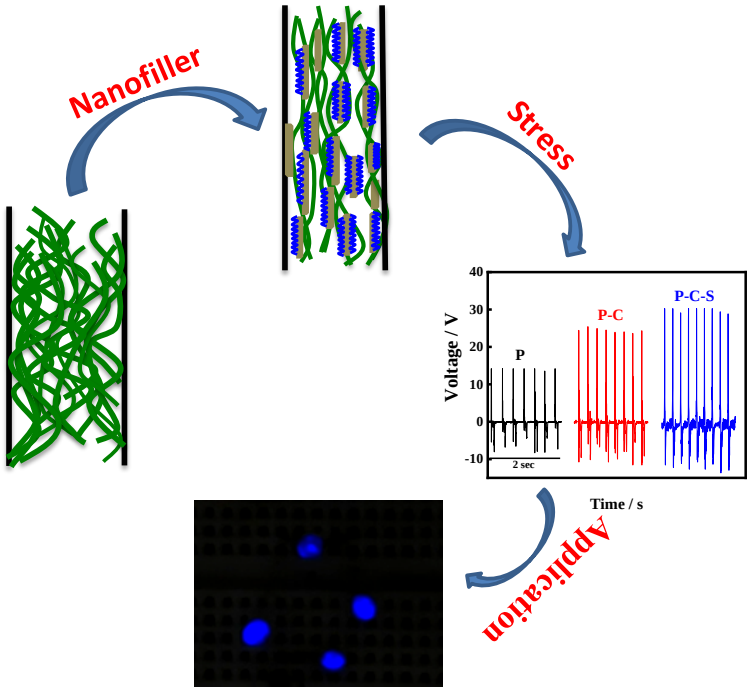

6.1 Introduction

Energy plays an important part in carrying out the needs of daily life efficiently. Most of the work performed throughout the day requires one or other form of energy. Being constantly dependent on the energy makes it the most vulnerable sources since most of the energy we consume is fulfilled by the conventional nonrenewable sources. The depletion of the present sources leads us to find an alternative source which may fulfill our needs with a sustainable future. Several alternate sources are being established and improvements are made which could provide a sustainable energy for the near future [78][25]. Energy harvesting is one of the alternate sources which are constantly upgraded for providing energy from different sources like waste mechanical source, vibration, acoustics, wind and many others. Waste mechanical energy to efficient electrical output is one of the areas which are continuously reviewed due to its scalability, environment friendly and easy availability and processablity [3][30]. Piezoelectric based energy harvesting is the most prominent and reliable one to generate energy from the waste mechanical energies to useful electrical output. It provides battery independent solution and is easy to use and an efficient source for low scale frequency based mechanical energies [93][128][129].The functionality and performance of these materials depends on its nature along with its processing techniques and fabrication methods. To harness such energy, several materials are processed and modified which could produce better energy efficiency. Inorganic materials like ceramics are the major attraction for piezoelectric energy harvesting because of their high piezoelectric properties as compared to the other materials. Piezo-ceramic materials like lead zirconate titanate (PZT) [123], barium titanate ($BaTiO_3$) [52], PMN-PT [184], ZnO [185] were extensively used for piezoelectric energy harvesting. Apart from the high piezoelectric properties of the piezo-ceramic materials they possess some limitations like

brittleness, rigidity, toxic and durability [24][136]. Hence to avoid such constraints, organic materials like polymers are sought which provide flexibility, durability, biocompatibility and better mechanical properties. Among the several polymers available, poly (vinylidene fluoride) or commonly abbreviated as PVDF and its copolymers have attracted the interest due to their advanced electroactive properties (piezoelectric, pyroelectric and ferroelectric), better mechanical strength, chemically stability etc. PVDF mainly consist of non-polar α-phase having TGTG′ conformations but possess the tendency to get transferred to piezo-active phases (β and γ) through some processing techniques like electrospinning, poling, stretching or electroactive filler addition. The β-phase PVDF (piezoelectric) is the main reason which makes the polymer most suited for energy harvesting applications. It possesses all trans (TTTT) conformation due to their structural alignment of $–CH_2$ and $–CF_2$ which leads to a net dipole moment in the system and makes it polar in nature. On the other hand, γ-phase is semi-polar in nature with $T_3GT_3\bar{G}$ conformations and possesses slightly lower piezoelectric properties than β-phase [130][93][35][96]. To raise the piezoelectric property of PVDF, piezoelectric fillers are sometimes added to widen its range of applicability. Several fillers like ceramic based materials such as PZT [89], $BaTiO_3$ [98], ZnO [141]; natural bio-based fillers like [107][109][62], fish scales[158]; 2D fillers like nanoclay [96][66] are used with PVDF for energy harvesting applications. Among the fillers used for such applications, carbon-based fillers are most extensively used due to their better electrical properties, high surface area, greater aspect ratio and good mechanical properties. Some of the commonly used carbon nanoparticles are graphene oxide, reduced graphene oxide, carbon nanotubes (CNT), carbon nanofibers etc. In the field of piezoelectric energy harvesting, carbon based fillers have their prominent roles and

several works based on polymer and carbon materials have been done and some remarkable outputs has been generated. The ease of designing and functionalization of these carbon materials makes them even more versatile [67][147][186][187][188]. Surface functionalization of these carbon based fillers leads to enhanced hydrophilic properties and better adherence which can be used for metal deposition for wide applicability [189]. Carbon nanofibers (CNF) are the newly introduced carbon materials due to its high surface to volume ratio and better electrical properties which is getting attracted and noticed by scientists and researchers for different applications. The smaller dimension and high aspect ratio of these nanofibers makes them suitable to be used along with polymer matrix to provide better mechanical strength and good electrical properties [190][191]. Despite its versatile properties, CNF or functionalized CNF are not much explored in the field of piezoelectric energy harvesting.

In this present work, functionalized CNF is prepared with sulphonating groups and is used as filler along with the CNF to form an electrospun polymer composite scaffold with PVDF. Electrospinning process is used to prepare the scaffolds which lead to self-poled and mechanically stretched samples. Functionalization of CNF enhances its dispersion ability and a well dispersed solution produces better quality of electrospun fibres. The effect of nanoparticles and functionalization on the piezoelectric energy harvesting applications is drawn out using different characterizations. The role of molecular structure and the effect of nanoparticle are studied using the computational study which correlates the experimental study from the theoretical perspective. The electrospun fibres are used to fabricate device which is used to measure the electromechanical responses against different

human motions. The ability of the fabricated device is analysed using different methods to understand its efficacy as a potential energy harvester.

6.2 Experimental

6.2.1 Functionalized carbon nanofibers synthesis: The functionalization of the carbon nanofiber is performed as stated in previous work [187][190].The CNF is sulfonated using ammonium sulfate. The CNF and ammonium sulfate was dispersed in DI water in the mass ratio 1:5followed by sonnication for 45 minutes. The sample was dried at 60-70^{o}C to remove the water from the mixture. Then the dried sample was heated at 245 ^{o}C for around 1 hour to allow the ammonium sulphate to decompose and form a $–SO_3H$ moiety in the surface of the fibres. The prepared functionalized CNF is abbreviated as CNF-S.

***6.2.2 Nanofiber preparation*:** The preparation of the polymer solution is discussed in chapter 2. The electrospinning was performed at the flow rate of 0.75 ml/h, 20 KV potential and 15 cm distance between collector and spinneret after performing certain optimization. The prepared scaffold was abbreviated as P, P-C and P-C-S for pure PVDF, PVDF and carbon nanofiber and PVDF and functionalized carbon nanofiber fibers, respectively.

***6.2.3 Theoretical / computational evaluation*:** In the context of the present work, the Gaussian 09 package is used for all electronic and thermodynamic calculations. Here, we studied all electron interaction within the Kohn-Sham implementation of the Density Functional Theory (DFT).From the previous literature, it is found that among the large number of approximation theories available, B3PW91 is a combination of the Becke's three-parameter (B3) exchange functional [191][192] and the correlation functional of Perdew and Wang (PW91) [193] produces the ground-state optimum equilibrium structures much more effectively. In this study, we use the B3PW91 level of hybrid theory assisted

with a 6-31G(d) [valence double x plus d polarization functions on heavy atoms] basis set to balance the accuracy and computational cost. All the structures were geometrically optimized and then were subjected to frequency calculations to obtain their thermochemical parameters. Later, the entire optimized polymer structures (both for α- and β- phases) are subjected to an applied external electric field of 500, 1000 and 1500 kV/cm. The change in geometrical, thermodynamic and electronic parameters are readily noted and the obtained values are studied thoroughly.

6.3 Results and Discussion:

6.3.1 Evidence of functionalization*:** To ascertain the addition of sulphonating group to the carbon chain of the carbon nanofibers, different characterizations are performed as shown in ***Figure 6.1.The schematic representation of the process of the sulphonation is depicted in the ***Figure 6.1a***. The FTIR spectra for the pristine CNF and functionalized CNF are shown in the ***Figure 6.1b***.The new peaks for S-CNF at 1198 cm^{-1} represents the -S=O stretching while the peak at 1402 cm^{-1} corresponds to the O=S=O group. The peak for C-S is seen at 619 cm^{-1} for S-CNF which is absent in the pristine CNF. Hence the generation of new characteristic peaks due to the addition of the sulphonating group in S-CNF from the FTIR study affirms that the sulphonating group is incorporated to the CNF [187][194][195][196]. ***Figure 6.1c*** shows the Raman spectra for the pristine CNF and functionalized CNF. The corresponding D-band which represents the disorder in the structure for CNF and S-CNF is seen at 1339 and 1343 cm^{-1}, respectively, while the G-band which arises due to the vibrational stretching of the C-C bond in the material occurs at 1561 and 1566 $cm^{-1}$for CNF and S-CNF, respectively. The subsequent shifting in the Raman spectra supports the functionalization of the CNF as seen from other techniques [195][197].Hence, the

functionalization of the carbon nanofibers is now evident from the different spectroscopic techniques.

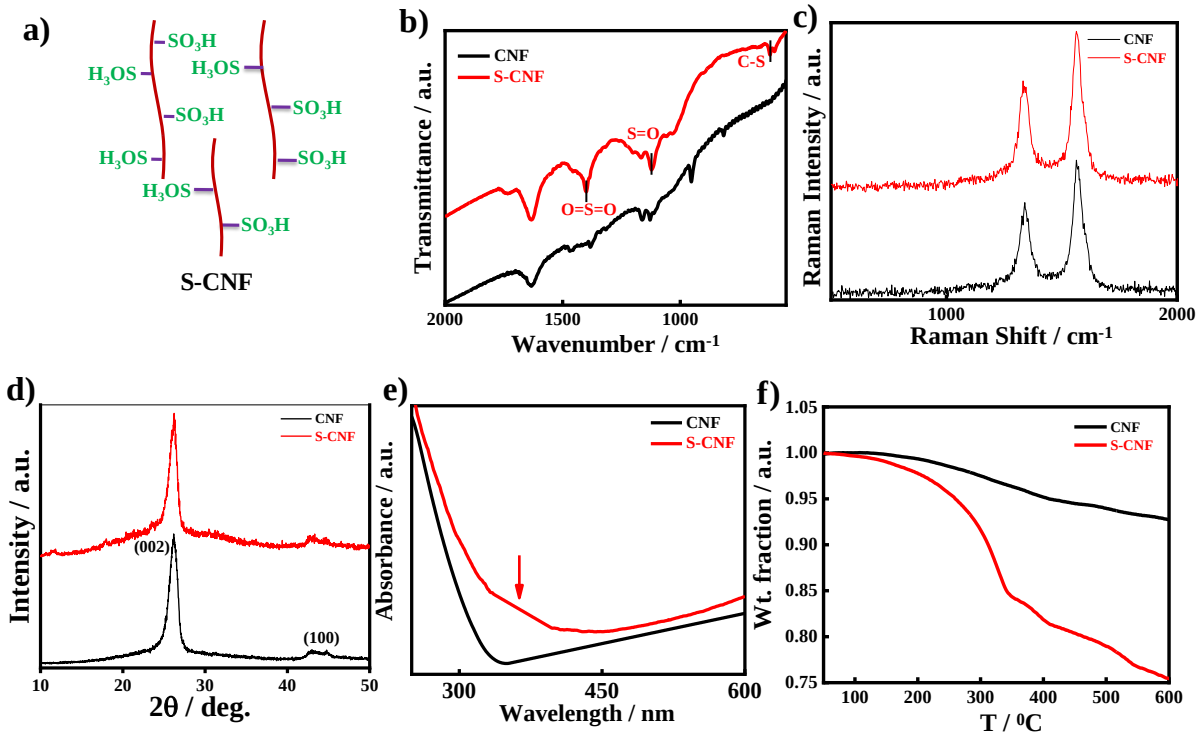

Figure 6.1: a) Schematic representation of the sulphonated carbon nanofiber; b) FTIR spectra for the CNF and S-CNF; c) Raman analysis for the CNF and functionalized CNF; d) XRD patterns of the CNF and S-CNF; e) UV-vis spectra of the CNF and S-CNF (arrow indicating the development of new peak for functionalized carbon nanofibers); and f) TGA thermogram for the CNF and S-CNF showing the variation in the thermal behavior due to the attachment of sulfonating group.

XRD diffraction pattern of the CNF and S-CNF is shown in ***Figure 6.1d***. In the neat CNF, two characteristic peaks are seen at 26.1 (002) and 42.9 (100) which represents the crystal plane of the graphitic layers and the turbostratic carbon plane, respectively. In case of the

S-CNF, the peaks get shifted to 26.3 and 43.2 which might be due to addition of the sulphonate group. A small broadening of the peak is seen in S-CNF and the broadness of peak may be attributed to the development of amorphous phase due to the addition of sulphonate group. Due to the sulphonation, the less ordered crystalline phase is developed as compared to the CNF which leads to slight broadening of the peak. The shift in the peak falls in accordance with the above characterization which affirms the functionalization of the nanofiller [198][199]. The functionalized carbon nanofiber was further analysed using UV-visible spectra (***Figure 6.1e***) which shows a new broad peak at 363 nm for S-CNF which may be due to the n-π* transition on incorporation of the sulphonate groups to carbon moiety, while no such peak is seen for pristine CNF. Hence, the UV-spectra support the attachment of the sulphonate group to the carbon chain of the carbon nanofiber. The thermal stability of the fillers is examined using TGA under the nitrogen atmosphere as shown in **F*igure 6.1f***. From the curve it is seen that the degradation of the S-CNF is rapid in the temperature range 180-350 °C as compared to the CNF and around 15% of degradation is seen at 350 °C which is due to the presence of the sulphonate groups attached to the carbon chain; whereas for CNF the rate of degradation is slower and around 5% degradation is seen at temperature 450 °C. Hence, for S-CNF, the presence of sulphonate group leads to a rapid thermal decomposition which is in accordance to results obtained in previous literature [200].

6.3.2 Effect of functionalization on the electrospun fibre:

The modification of the carbon nanofiber with the sulphonate group is impregnated to the polymer matrix and its effect on the fibre morphology is studied using the SEM technique as shown in the ***Figure 6.2a-c***. From the SEM images it is seen that the addition of the

functionalized CNF (S-CNF) to the PVDF matrix leads to a better fibre as compared to the pristine polymer. In the pure PVDF fibre, the presence of beads is seen which appears from the non-polar phase of the polymer which is not transformed to the polar phase during electrospinning. The fibre quality is improved for P-C (composite with untreated CNF) with the reduction in bead content and almost no bead formation is seen in P-C-S (composite with functionalized CNF). The presence of electroactive filler imparts charge during the electrospinning process which results in reduced beads content as compared to the pure polymer. Due to the modification of the CNF, the dispersion of the filler gets better which results in even better fibre quality with minimal bead content. Hence, the functionalization of the filler impregnates better fiber morphology which is the indicative of the transformation of the non-polar phase to polar phase. The fibre diameter using the SEM micrographs is shown in the ***Figure 6.2d***. The average fiber diameter for the P and P-C-S is around 250 ± 10 and 210 ± 7 nm, respectively. Addition of the electroactive filler to the PVDF matrix leads to better interaction and due to the columbic force and electrostatic repulsion because of presence of electroactive filler better fibre are obtained with thinner dimensions. The functionalized carbon nanofibers having the presence of sulphonate group increase the charge density in the solutions, as a result better dispersion of the filler is possible due to enhanced dipolar interactions between the filler and the matrix, and thus, better quality fibres are generated through electrospinning. [187][65]

The role of functionalization on the structure is investigated using the XRD diffraction pattern. ***Figure 6.3a*** shows the XRD patterns of the pristine polymer and its nanohybrids. It is evident that the addition of the electroactive fillers leads to transformation of the non-polar α-phase to polar β-phase. The XRD pattern for P (pure PVDF fibre) shows three

characteristic peaks at 18.4° (020), 20.15° (200/100) and 26.6° (021). The peak at 18.4° and 26.5° is attributed to the non-piezo α-phase while the peak at 20.15° resembles the β-phase. Addition of CNF to the polymer matrix leads to the diminishing of the α-phase peak and the β-phase peak shifts to higher 2θ value of 20.4°.

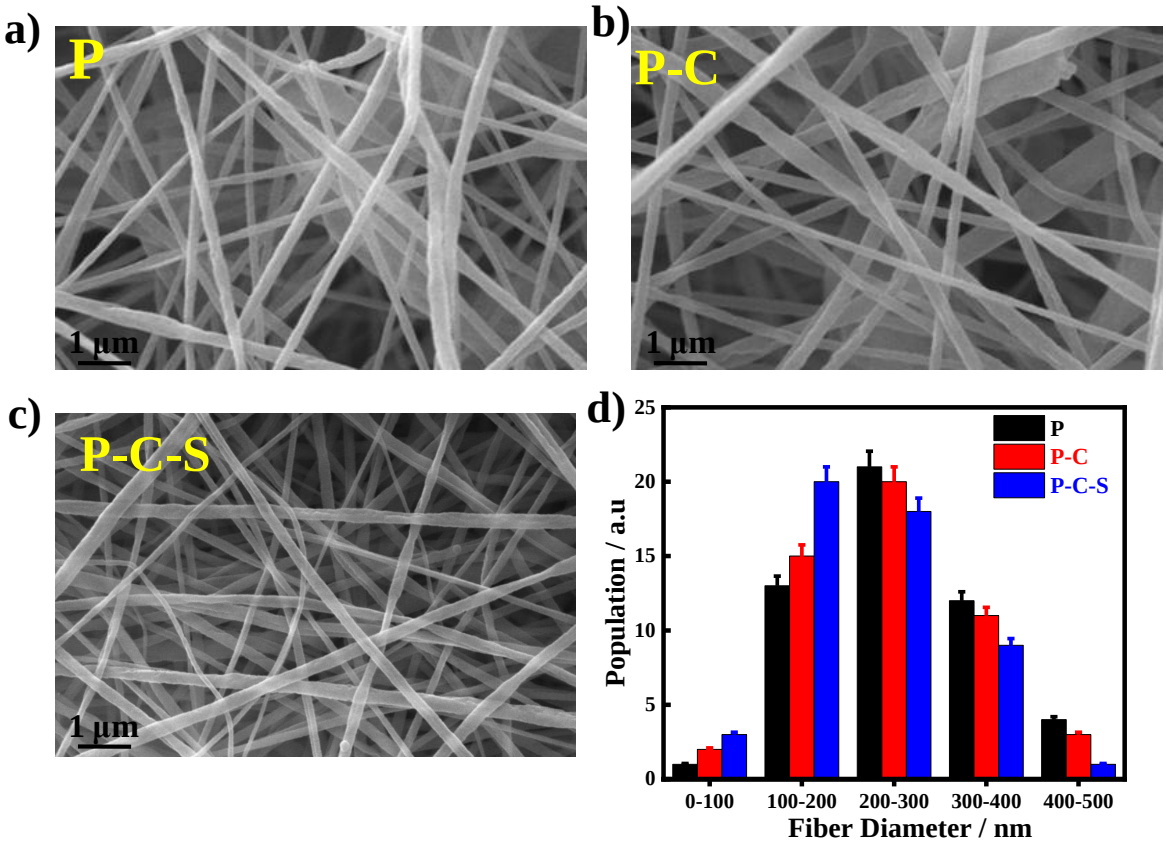

Figure 6.2: SEM micrographs of the electrospun scaffolds of a) P; b) P-C; c) P-C-S; and d) the fiber diameter distribution from SEM images of electrospun fibers as indicated.

Addition of the functionalized CNF to the PVDF further reduces the α-phase peak and a single intense peak which signifies the polar β-phase is obtained at 20.46°. The shift in the 2θ value of the β-phase and the diminished non-polar phase peak suggests the better interaction of the filler with the polymer matrix. The functionalized CNF induces higher

electroactive phase as compared with the pristine CNF due to the better dispersion and interaction. [96][50] The better quality fibres obtained from the functionalized CNF leads to better polar structure which suggests its importance as piezoelectric material for energy harvesting applications. The phase fraction obtained from the deconvolution of the XRD peaks as shown in ***Figure 6.3b*** exemplifies the transformation of the non-polar phase to piezo active phase which is evident from the rise in the electroactive phase (β-phase and γ-phase) and the decrease in the α-phase content. The maximum content of piezo-active phases for P, P-C and P-C-S are around 66%, 73% and 85%, respectively. The rise in the content of the electroactive phase supports the observation from the XRD curve and signifies the role of addition of electroactive fillers to the polymer matrix as a suitable material towards the piezoelectric energy harvesting applications.

The structural changes is further analysed using the FTIR spectra as shown in the ***Figure 6.3c***. The peaks obtained for the P is 975, 796, 760, 613 cm^{-1} which are the main characteristic for the α-phase while the peaks at 1277, 1182, 1069, 876 cm^{-1}signify the β-phase generation. When the CNF and S-CNF is impregnated to the PVDF matrix, it leads to attenuation of peak and the α-phase peaks gets diminished which suggests the phase transformation from non-polar phase to the polar phase. The β- phase peaks get shifted to 1278, 1181, 1072 and 881 cm^{-1} for P-C-S. The confirmatory peak for γ-phase is seen at 1241 for P-C and 1238 for P-C-S. Hence, the addition of the CNF and S-CNF leads to the transformation of the non-electroactive phase to electroactive phase which is in accordance with the results obtained from previous characterization techniques.[201][101]

Raman spectra confirm the presence of structural changes as seen in ***Figure 6.3d.*** Neat PVDF fibres show characteristic peaks at 610, 790, 835 and 880 cm^{-1} which gets attenuated

and shifted in case of the nanohybrids. The peak at 610cm^{-1} is due to the -CF_2 vibrations which get diminished for P-C-S; also the intensity of peak at 790 cm^{-1}is reduced in P-C-S as compared to P which suggests the structural transformation of the non-polar part to polar part.

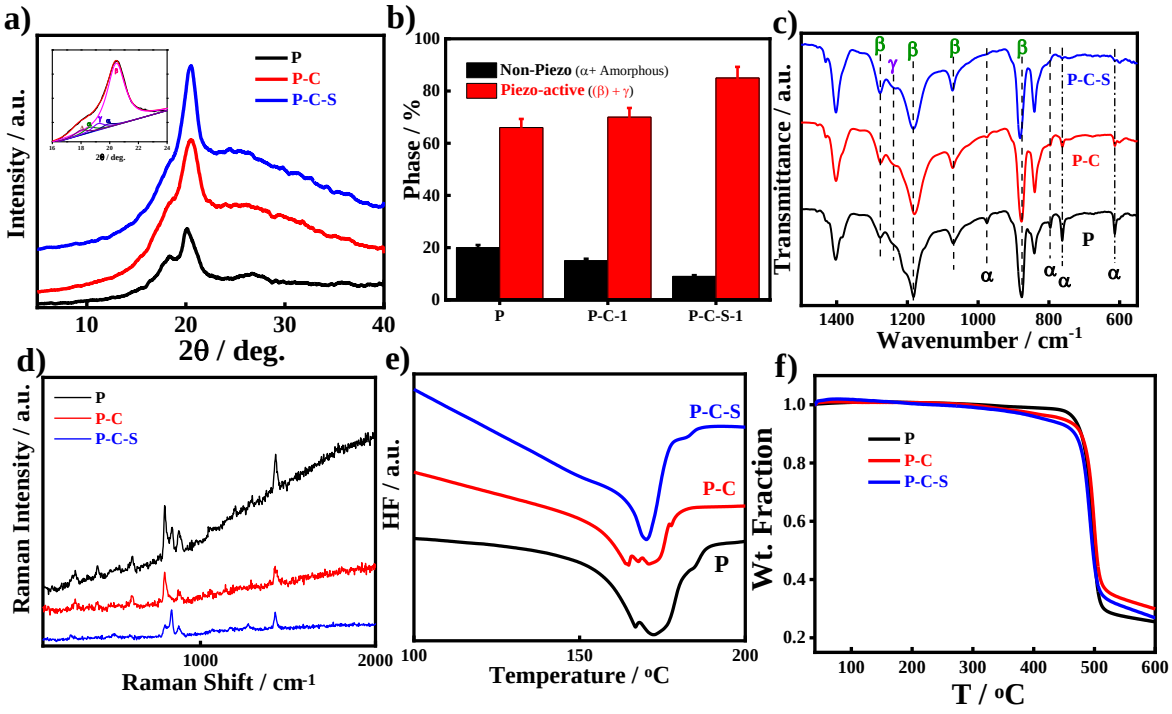

Figure 6.3. a) XRD patterns of the electrospun scaffolds of PVDF and its nanohybrids (inset showing the deconvolated representation of the XRD peaks); b) estimated phase fraction of the piezo (β and γ together) and non-piezo phases from the deconvolated XRD curve; c) FTIR spectra of pure PVDF and its nanohybrids indicating the different phases; d) Raman spectra of P, P-C and P-C-S; e) DSC thermograms of the electrospun nanofibers of P, P-C and P-C-S representing the change in the melting temperature with the filler incorporation; and f) TGA curves of PVDF and its nanohybrid fibres.

The peak observed around 836 cm^{-1}signifies the out of phase arrangement of -CF_2 stretching and -CH_2 rocking modes. These modes are mainly for the polar phases (β / γ) in the PVDF based nanohybrids. A common peak is observed around 1432cm^{-1} which is due to the -CH_2 vibrations present in all three phases of PVDF. Hence, the observation drawn from the Raman spectra validates the results obtained from XRD and FTIR, confirming the development of piezo-active phase upon incorporation of the nanofillers [197][202].

Differential scanning calorimetry is also used to confirm the development of the polar phases upon incorporation of the electroactive fillers, as shown in the ***Figure 6.3e***. The pristine PVDF shows melting peaks at 166.8 °C and 172.3 °C which are the characteristic peaks for the β and α phase, respectively. For P-C-S, due to better interaction of the S-CNF with the polymer matrix, a sharp peak is seen at 170.1°C which is the nearly complete transformed peak of the β-phase suggesting the importance of the functionalization of the filler on the phase transformation. Also a peak around 182.3 °C is seen which suggests the melting of the semi-polar γ-phase (higher melting peak). Hence, the melting temperature seen of different phases is in accordance with the results obtained in literatures and follows the order β < α < γ [94][96][67]. The observation made from the DSC thermographs supports the results obtained from XRD and FTIR study and hence, confirms the role of electroactive filler addition to the polymer matrix in transforming the non-polar phase to the polar phases. The thermal stability of the electrospun scaffold is analysed using the thermogravimetric analyser as shown in the ***Figure 6.3f***. The thermal stability is considered under the uniform heat treatment and the corresponding temperature to 5% of weight loss is considered as the degradation temperature. The observed degradation temperature (5% of weight loss) for P (pure PVDF fibre) is around 465 °C which on addition of the CNF and

S-CNF to the PVDF occurs at 450 and 420 °C, respectively [200][181][203]. Therefore, the addition of nanofillers to PVDF matrix leads to the reduction in the degradation temperature which may be attributed to the better dispersion of the nanofiller as compared to the virgin PVDF fibre. [97] When a piezoelectric active nanoparticle is added to the polymer, it leads to the enhancement in piezoelectric properties and also behaves as a nucleating agent which results into the stretching of the fibers because of better electrostatic interaction between polymer and fillers. It is evident from the structural and thermal alterations that the addition of the electroactive nanoparticles to the polymer moiety leads to rise in piezoelectric phases which may be attributed to the nucleation and crystallization of nanoparticles onto the polymer matrix which results in the better alignment and piezoelectric properties [204].

6.3.3 Theoretical and computational perspective of phase transition:

A schematic representation shown in ***Figure 6.4a*** highlights the role of nanofiller to attain better alignment and hence generates enhanced electroactive phase which clarifies the potential of the material as a better piezoelectric energy harvesting material. When nanofillers are incorporated to the PVDF matrix, the alignment of the nanofibers gets better in addition to the nucleating effect of the reinforcing agent which generates better quality of fibres that leads to enhanced piezoelectric properties. To understand the effect of the molecular structure and the nanoparticle, computational study has been carried out which provides the clear view of the mechanism which leads to the enhanced piezoelectric properties. To get a broader idea on the interaction of the nanoparticle with the polymer matrix, computational study using Gaussian and Density Functional Theory (DFT) is performed which clarifies the role of electroactive phases and effect of nanofillers on the

enhancement of the physical properties. DFT is one of the most common and powerful technique used to elucidate and understand the ground state electronic properties of the materials. In case of polymeric materials, DFT is an effective method because of its capability to include most of the electronic correlations in case of moderately large molecules [205][206][207]. To understand the role of molecular configuration, PVDF chains with 2 to 7 monomer units is being studied for the PVDF-α chain with $TGT\bar{G}$ and PVDF-β chains with all trans TTTT configuration. ***Figure 6.4b*** shows the representation of the molecular configurations of pure PVDF (α and β) with 3 and 7 monomer units. The optimized results indicate that the average distances of adjacent monomer units in case of a 7-monomer unit chain are 2.6 and 2.5 Å for α and β-phase, respectively. These values are in excellent agreement with the experiment value of 2.56 Å obtained from X-ray diffraction study [208]. However, with respect to the increase in chain length there is a slight but consistent decrease in adjacent monomer distance. In case of β-PVDF, the average distance of adjacent fluorine couple is around 2.7 Å where as the distance for hydrogen couples are ~ 2.4 Å i.e. smaller than the fluorine couples, thereby predicting the bending nature of polymer chain into a circular structure. The above results are in good agreement with the previous study by Wang. et. al. [209]. PVDF is a polymer which has the ability to get transformed to the polar phase on the application of external factors like electric field due to the alignment of the dipoles which results into the net dipole moment that leads to better piezoelectric properties. Depending upon the conformation and molecular aggregation, dipole moment and polarizability are the important properties for the electroactive materials.

The change in the dipole moment with the number of monomer unit is shown in ***Figure 6.4c***. The average dipole moment (without electric field) for the α-PVDF is around 5.41× 10^{-30}C.m while that for the β-PVDF is ~ 7.02 × 10^{-30} C.m which is in accordance with previous works [210]. The rise in the dipole moment suggests the effect of alterations in molecular conformation which leads to enhanced piezoelectric properties. From the curve, it is seen that with the increase in the monomer unit the dipole moment per unit monomer decreases. The dipole moment in the individual unit of monomer is perpendicular to the polymer chain but on increasing the monomer unit the chain length rises which leads to curving of the chain due to electrostatic repulsion of the fluorine atoms. [211]

The effect of the electric field is clearly seen which confirms the effective increase in dipole moment under prior electric field. ***Figure 6.4d*** represents the curve depicting the change in polarizability with the monomer units in absence and presence of electric field. The average polarizability (without electric field) for α-PVDF and β-PVDF is 40.42 × 10^{-41}C m^2 V^{-1} and 40.90 × 10^{-41}C m^2 V^{-1}, respectively. The polar nature of the β-PVDF results in the rise in the average polarizability which supports the values obtained from the dipole moment analysis. On application of the external electric field to the PVDF chain, the value of the polarizability increases as shown in the curve.

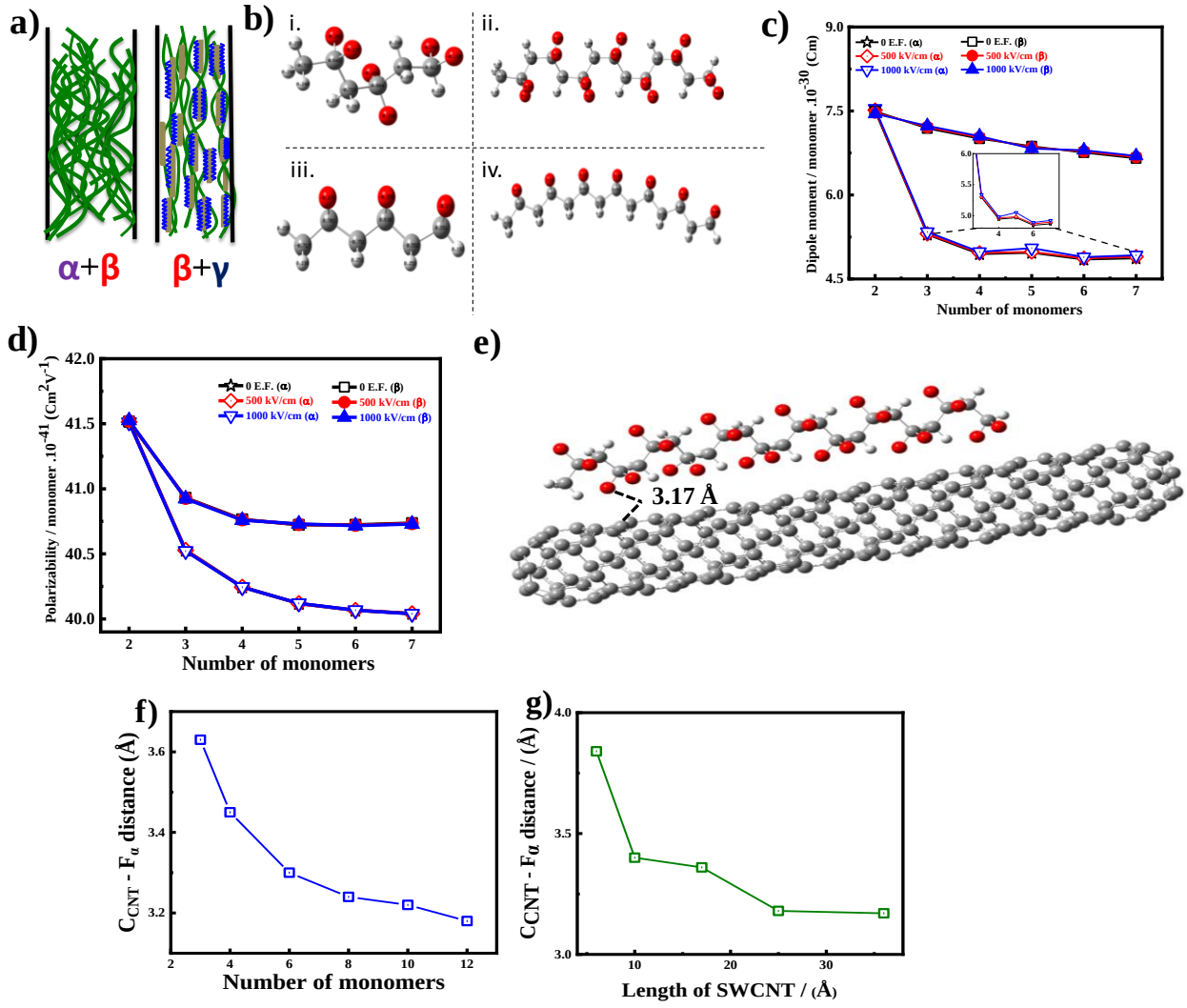

Figure 6.4: a) Schematic representation of the effect of nanofiller to generate better quality fibers with better piezo-phase formation (grey rod type structure indicated the S-CNF which facilitates nucleation); (b)The optimized structures showing Mulliken charge distribution of (i) α-PVDF (3 monomer) (ii) α-PVDF (7 monomer) (iii) β-PVDF (3 monomer) and (iv) β-PVDF (7 monomer); (c) dipole moment per monomer unit vs. PVDF chain length (inset shows the extended curve for a range of monomer unit showing the changes significantly); (d) average polarizability per monomer unit vs. PVDF chain length; e) optimized structure of the PVDF (12 monomer unit) with CNT (36 Å)showing the

minimum distance between the PVDF and CNT; f) minimum distance between the C (CNT) and F (PVDF) as a variation of monomer unit of PVDF on the fixed CNT (25 Å) length; and g) change in minimum distance between the F (PVDF) and C (CNT) on varying the CNT length for a fixed PVDF monomer units (12).

When an electric field is applied on to PVDF chain, the alignment of the molecules takes place, occurs due to the rotation of the hydrogen or fluorine atoms, as a result provides a net dipole moment to the system and hence, increases the piezoelectric properties [212]. When electrospinning is performed, high electric field is provided to the polymer solution which in combination with the stretching leads to better alignment of the molecules and generates a net dipole moment into the system that leads to enhanced electroactive properties. Therefore, the experimental and the computational observation stand in line and conclude the role of electric field and molecular conformations for better piezoelectric properties.

To understand the effect of the filler, computational analysis is performed using different monomer unit of PVDF and the variable length of the CNT. Since, carbon nanofiber represents one dimensional filler, to ease the theoretical evaluation, CNT is being considered which is the widely used one-dimensional filler. The interaction between the CNT and PVDF is performed using the geometrical optimizations. All the structures were relaxed using BFGS type of hybrid theory without any fixed symmetry constraints. ***Figure 6.4e*** shows the minimum distance between the PVDF and CNT after the structural optimizations and evaluation. The calculation is performed over the CNT with the length of 36 Å and over 12 numbers of monomers for PVDF. The minimum distance between the carbon atoms of the CNT (C_{CNT}) and the fluorine atoms of the PVDF (F_{α}) monomer is 3.17

Å. The optimized structure reveals that on adding the CNT to the polymer matrix the electrostatic interaction leads to the decrease in the distance between the CNT and PVDF. The addition of electroactive fillers generates better interaction with the PVDF which results in enhanced piezoelectric properties. To analyse the effect of the monomer size and the CNT length variation on the distance between the CNT and the PVDF monomer unit, different number of monomer units and the varying CNT length have been studied. ***Figure 6.4f*** represents the change in the minimum distance between the fluorine atom of PVDF unit and the carbon atom of the CNT. The length of the CNT was fixed at 25 Å while the number of monomer units was varied. From the curve it is seen that on increasing the number of monomer unit the minimum distance between the C_{CNT} - F_{α} reduces which might be attributed to the enhanced interaction with the polar F-group and also due to the coiling of the PVDF chain on raising the number of monomer unit. On altering the case with the CNT length and monomer unit, ***Figure 6.4g*** shows the changes in the minimum distance between the C_{CNT}-F_{α} on varying the CNT length at fixed monomer unit of the PVDF (12 monomer units). The results obtained from the analysis suggest similar observation as from the previous curve (***Figure 6.4f***). On increasing the length of the CNT, the distance between the C_{CNT}-F_{α} reduces which suggests that CNT addition leads to better interaction with the PVDF moiety. On comparing the values of dipole moment and polarizability of the α-PVDF, β-PVDF and α + CNT (CNT of 25Å length) as shown in the ***Figure 6.5***, it is seen that the values of the dipole moment and the polarizability for α + CNT lies between the values of the α-PVDF and β-PVDF suggesting the transformation of the non-polar part to the polar part in presence of the electroactive filler CNT. The dipole moment values for the six monomer unit for α-PVDF, α + CNT and β-PVDF is 4.84, 5.00 and 6.75 × 10^{-30}

C.m, respectively. Similarly, the polarizability values for the α-PVDF, α + CNT and β-PVDF is 40.06, 40.37 and 40.72 × 10^{-41} Cm^2V^{-1}, respectively. However, it can be concluded from the computational approach that addition of the electroactive filler (functionalised CNT) leads to enhanced properties due to better interaction with the PVDF matrix which is in accordance with the results obtained from the experimental analysis.

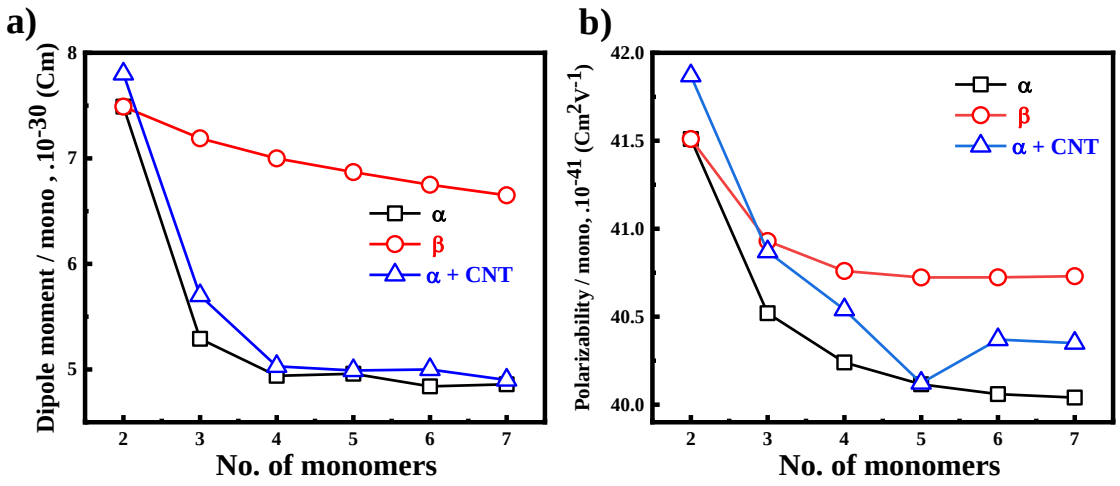

Figure 6.5: Computationally calculated values of a) dipole moment / monomer and b) polarizability / monomer for α-PVDF, β-PVDF and α + CNT.

6.3.4 Functionalized filler induced piezoelectricity and its applications:

Now it is relevant to discuss the piezoelectric effect of the electrospun scaffolds of PVDF and its nanohybrids after the observation drawn from the structural, morphological and thermal studies in ***Figure 6.1 and 6.2***. From the above figures it is evident that the addition of nanofiller especially the functionalized nanofiller imparts better piezo-phase to the material as compared to the pristine polymer. Moreover, based on the above observation, the electromechanical properties and responses are being carried out to understand the

efficacy of the device fabricated from the electrospun scaffold under different modes. The device designed from the electrospinning of the PVDF and its nanohybrids consists of four parts: scaffold, aluminum substrate, copper wires as electroding materials and poly(dimethyl siloxane) (PDMS) as encapsulating material. To impart better stability and uniformity to the prepared material, PDMS is used. The fabricated device is subjected to various stresses to understand its efficacy as piezoelectric energy harvester. A piezoelectric nanogenerator produces certain response on application of the external pressure. When an external force or stress is applied to the device, the deformation in the structure takes place which may be attributed to the change in the crystal arrangements and thus, the alignment of the dipoles becomes anti-parallel resulting into a net dipole moment of the system. When a stress is applied onto the fabricated device via different modes, the pressure is distributed along the material as a result charge gets separated and a net flow of charge flows through the external circuit. On imparting and releasing pressure to the nanogenerator, a potential difference between the electrodes is developed which leads to generation of substantial electromechanical response. When no stress is applied or strain is kept constant, no flow of charges takes place, as a result there is no generation of any dipole moment and therefore no voltage difference is observed along the circuit. [123][3][106] ***Figure 6.6a*** depicts the piezoelectric coefficient value (d_{33}) of the prepared scaffolds. The value obtained for the neat PVDF fibre is -5 pC / N which rises substantially to -10 pC / N and -14 pC / N for P-C and P-C-S fibres, respectively. The increase in the value of the d_{33} with the incorporation of the electroactive fillers can be attributed to the better fiber alignment due to good electrostatic interaction between the fillers with the polymer matrix. [101] ***Figure 6.6b*** represents the generated output voltage through finger tapping mode on the fabricated

device using P, P-C and P-C-S fibres. The maximum output voltage generated (peak-to-peak) from P is around 22 V which gets enhanced to 35 V and 44 V for P-C and P-C-S systems, respectively. The rise in the output voltage can be related to the structural transformation as seen from ***Figure 6.2***. Addition of nanofiller to the PVDF matrix leads to better electroactive phase formation which further enhances the piezoelectric properties. When a mechanical force is applied onto the nanogenerator, the charge generated flows back and forth between the electrodes and thus an electric polarization is induced onto the system. When pressure is applied positive signal is generated while on the release of the pressure the charge accumulated near the electrode flows back to the other electrode and a negative signal is generated. [156][60]

The power generated from the device is calculated using the following relation [107]:

$$\mathbf{P_d = V_o^2 / (R \times A)} \qquad \mathbf{(6.1)}$$

where, P_d is the power density across the material, V_o is the output voltage, R is the resistance across which the voltage is measured and A is the area of the active material. The maximum power density measured across the fabricated devices are around 21.4, 27.8 and 36.7 $\mu W cm^{-2}$ using P, P-C and P-C-S fibres, respectively, using the above equation 6.1 (***Figure 6.6c***). The rise in the power density value is in accordance with the output voltage generated and therefore, supports the effect of filler and its functionalization on the electromechanical responses.

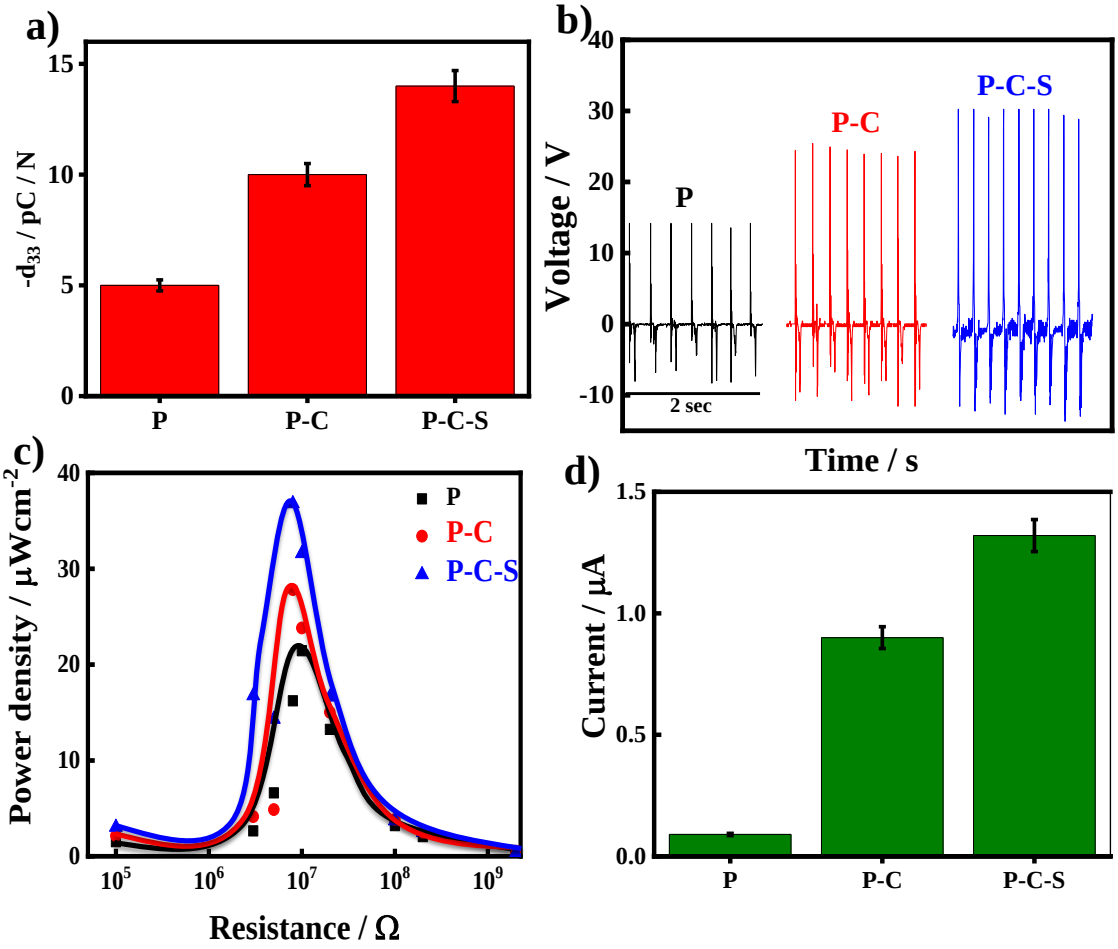

Figure 6.6: a) Piezoelectric coefficient (d_{33}) values for P, P-C and P-C-S as indicated; b) output voltage generated through finger tapping mode from the fabricated devices using the electrospun scaffolds of P, P-C and P-C-S; c) power density plot w.r.t. resistance for the neat PVDF and its nanohybrid fibres; and d) output current obtained from finger tapping mode from the devices using P, P-C and P-C-S fibres.

Zhao et.al [196] developed a nanogenerator from PVDF-TrFE / MWCNT and the maximum output voltage and power density achieved was around 18.23 V and 6.53 μWcm^{-2}, respectively. Alluri et.al [131] prepared the composite of PVDF-activated carbon and obtained the maximum output voltage and power density of 37.8 V and 6.3 μWcm^{-2},

respectively. The finger tapping mode was used to measure the current using the digital multimeter as shown in ***Figure 6.6d***. The maximum current generated for P, P-C and P-C-S is around 0.09, 0.9 and 1.3 μA, respectively. The increase in the current with the addition of the electroactive filler is in the support with the output voltage and power measured. Using the output voltage (peak-to-peak) and the current produced, power can be calculated using the relation:

$$P = V \times I \qquad (6.2)$$

Thus the maximum power obtained using the equation 2 for P, P-C and P-C-S devices are around 1.98, 31.5 and 57.2 μW, respectively.

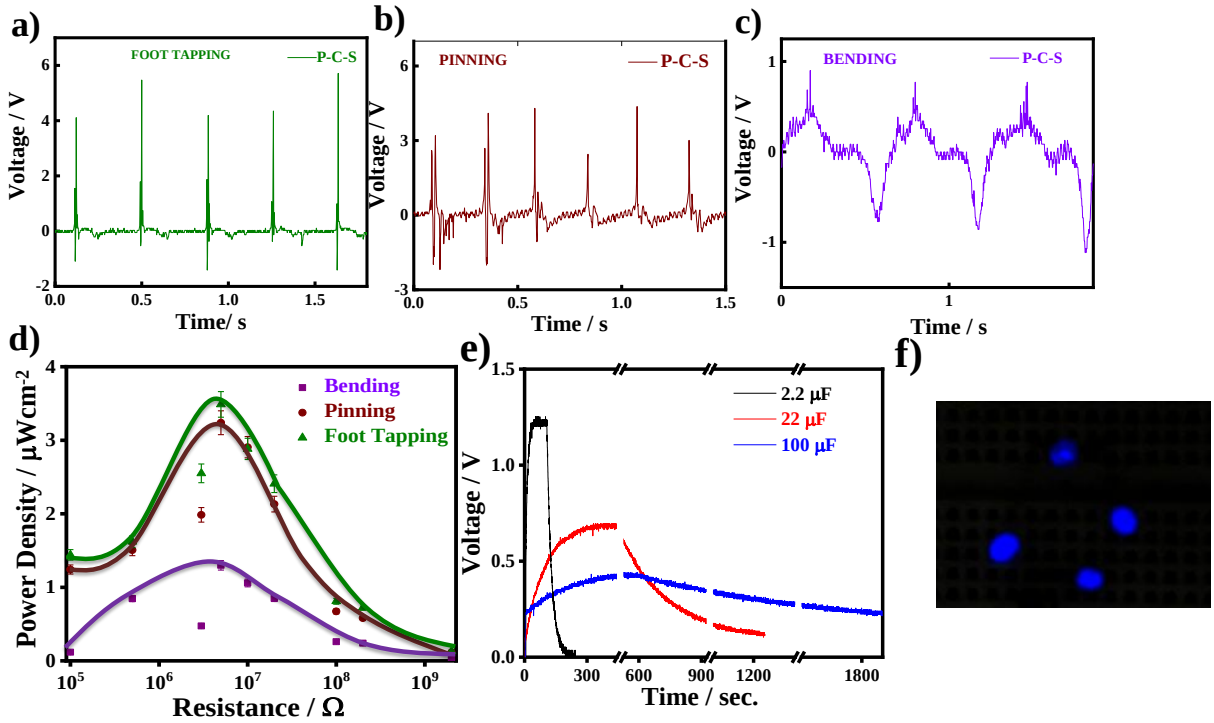

Figure 6.7: Generated output voltage from a) foot tapping mode; b) pinning with glass slide; c) bending mode on fabricated device; d) power density plot against load resistance

for the different modes as indicated; e) charging – discharging phenomenon for P-C-S at different capacitor ratings using an external load and f) pictorial view of illuminated LEDs from the finger tapping mode.

The device is further used to harness energy from different mechanical sources from different human body movements and external pressure to understand its role as efficient energy harvester. ***Figure 6.7*** shows the open voltage (peak-to-peak) generated and power density obtained from P-C-S fibre device from different motions like bending, pinning and foot tapping. Bending of the nanogenerator produces maximum output voltage of around 2 V (***Figure 6.7a***), pinning of the device (***Figure 6.7b***) with single glass rod generated around 6.3 V (peak-to-peak) and foot tapping (***Figure 6.7c***) on the device led to maximum potential of 7.1 V. Power densities measured across the resistance for bending, pinning and foot tapping (***Figure 6.7d***) are around 1.3, 3.2and 3.5 μWcm^{-2}, respectively. To investigate the device's applicability for storage application, the device was subjected to an external pressure connected through full bridge rectifier circuit to analyse the charging – discharging phenomenon on different ratings of the capacitors as shown in ***Figure 6.7e***. The accumulated voltages for the capacitors of 2.2, 22 and 100 μF are around 1.24 V, 0.70 V and 0.45 V, respectively. When external stress is applied onto the device, it stores charge in the form of output voltage generated from the device connected to the capacitor through the bridge rectifier and on attaining saturation, when no external pressure is given discharging phenomenon takes place. Based on the curve obtained from the charging-discharging process, it is evident that the device is able to store charge on the application of external stress. [60][65]

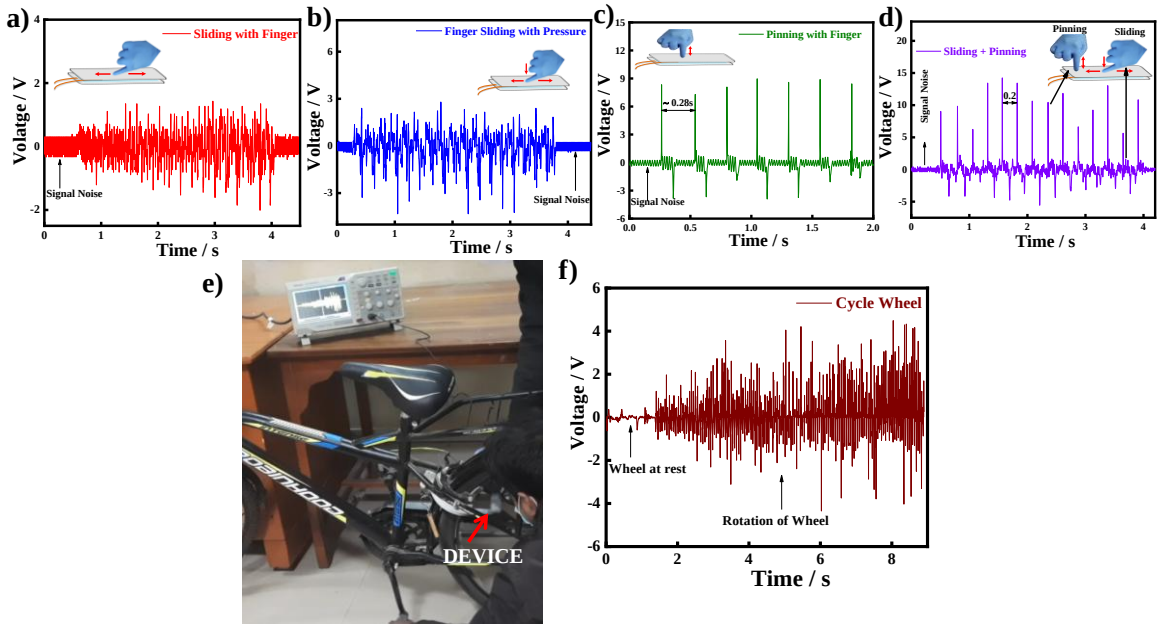

Figure 6.8: Tribological pressure based output voltage curves against time through a) sliding with finger with minimal pressure; b) sliding with finger with some pressure; c) pinning with finger; d) combined process of pinning and sliding with pressure; e) a set up demonstrating the applicability of the device when subjected to the rotating bicycle wheel; and f) output voltage generated from the device when subjected to external pressure from hitting of rotating bicycle wheel spokes.

Now, it is conclusive that the prepared scaffolds lead to considerable amount of voltage and power, being harnessed from the fabricated device which describes the efficacy of the material as a piezoelectric energy harvester. Demonstrating the practical applicability of the fabricated device, the device is able to light up some LEDs and charge up the capacitor on the application of the external pressure through finger tapping. A screenshot of the LED glowing on impact of finger tapping is shown in ***Figure 6.7f*** which clearly reveals the efficacy of the fabricated device. Hence, it is now conclusive that the electrospun scaffold

of the neat PVDF and its nanohybrid is a superior material for piezoelectric energy harvesting based on the morphological, structural, thermal and electromechanical analyses.

To explore the better applicability of the fabricated device, tribological mode (behavior of the device with respect to relative motion) is used to analyse its response. In the ***Figure 6.8 a-d*** some output signals in terms of voltage against time is shown. ***Figure 6.8a*** shows the output voltage (peak-to-peak) of 3.4 V when a finger is slided over the surface of the device without applying much pressure on the device. The force applied over the surface of the device is from the human finger. On applying pressure while sliding over the device surface, substantial increase in the output voltage (peak-to-peak)(7 V) is seen (***Figure 6.8b***). Also it can be visualized that on applying sliding force,the nature of the signal is almost continuous without much gap between two signals and which is higher than the base signal noise as shown in the curves. Thus it is affirmed that the applying relative force or pressure over the device generates considerable amount of output voltage. The device is then subjected to finger pinning as shown in ***Figure 6.8c*** which results in maximum output voltage (peak-to-peak) of 12.9 V. The time interval between two signals is almost around 0.28 seconds. In the case of finger pinning, the continuity of the signal is periodic. In ***Figure 6.8d***, a combined effect of finger pinning and finger sliding is demonstrated in the inset of the curve which leads to a better response than the other tribological modes. The maximum output voltage (peak-to-peak) obtained from the combined mode is around 18.7 V. The time interval for the two signal peaks gets reduced to ~ 0.2 seconds as compared to the ~ 0.28 seconds for finger pinning. Also from the curve, it is evident that almost a continuous signal is produced throughout the measurement which is a better outcome for the field of energy harvesting where a continuous signal output is a boon for nanogenerator

applications. When sliding and pinning is applied onto the device continuously, the generation of charge is constantly produced which leads to a continuous signal production higher than the signal noise when no pressure is applied to the device. Hence the tribological study demonstrates a continuous method to generate output electrical signal by reducing the time interval between the two signals and provides a mechanistic path for a continuous generation of charges on application of external pressure. The designed device is placed between the spokes of a bicycle wheel to analyse the practical applicability of the material. ***Figure 6.8e*** shows the setup designed for the measurement. The device is placed near the spokes of the wheel and on peddling of the bicycle wheel leads to hitting of the device which acts as an external pressure and on hitting an output is generated which is measured through the DSO. The maximum output voltage (peak-to-peak) generated as shown in ***Figure 6.8f*** is around 8V which is a substantial amount of response and hence the efficacy of the device is clearly understood as a potential material for piezoelectric energy harvesting applications. In brief, an important class of carbon compound, carbon nanofiber, is suitably functionalized through chemical means which interact with polymer matrix efficiently and induces piezoelectric phase in the polymer appropriate for its application in energy harvesting. Device has been designed which exhibit power generation in sufficient quantity by utilizing the waste mechanical source arising from the body movements and other conventional wastage of mechanical power like bicycle.

6.4 Conclusion

Electrospun nanofibers of PVDF, carbon nanofibers and sulphonated carbon hybrid nanofibers are developed using the electrospinning process. The addition of the sulphonating moiety to the carbon chain of the carbon nanofiber is evident from different

techniques. The functionalization of the carbon nanofiber led to better dispersion and interaction of the carbon nanofiber with the polymer matrix. The addition of the electroactive filler and its functionalized counterpart to the polymer matrix generate better quality fibres as compared to the pristine PVDF fibers which are confirmed from the structural as well as morphological studies. The addition of the functionalized CNF leads to thinning of fibers diameter due to better electrostatic interaction of the filler with the polymer. The structural and thermal studies confirm the transformation of the non-piezo phase to piezo-active phase with maximum electroactive phase content of ~ 85 % for P-C-S(functionalized hybrid) as compared to ~ 66 % for P (pure polymer fibre). The ability of the nanofiller to convert the non-polar fraction to polar component makes the hybrid fibre a potential piezoelectric material which can be used for the energy harvesting applications. The device designed from the prepared scaffold is used to observe the electromechanical response from different motions or external pressure. Maximum output voltage (peak-to-peak), current and power density generated from P-C-S are around 44V, 1.3 μA and 57.2 μW, respectively, which are much higher as compared to the pure PVDF fibre (22V, 0.09μA and 21.4μWcm^{-2}). The functionalization of CNF with sulphonating group enhances the dispersion and interaction of the filler with the polymer matrix which results in the better fiber quality with higher response against mechanical pressure. The device is also able to generate considerable energy from the different motions of the human body like bending, pinning and foot tapping which supports the efficacy of the material to generate substantial output against minimal load applied to the device. Tribological study supports the efficacy of the device when subjected to a relative motion type of external pressure generating a continuous signal with reduced signal gap. Thus, the electrospun PVDF

nanohybrids produce better piezoelectric responses when functionalized CNF is added as filler generating better power and voltage output and producing substantial response when subjected to different external motions demonstrating the practical applicability of the developed device.